Proc. Natl. Acad. Sci. USA
Vol. 92, pp. 2622–2626, March 1995
Pharmacology

Rapid endocytosis of a G protein-coupled receptor: Substance P-evoked internalization of its receptor in the rat striatum *in vivo*

(substance P receptor/neurokinin 1 receptor/central nervous system/desensitization/receptor-mediated endocytosis)

PATRICK W. MANTYH*†‡, CLARK J. ALLEN*†, JOSEPH R. GHILARDI*†, SCOTT D. ROGERS*†, CHRISTOPHER R. MANTYH§, HANTAO LIU¶, ALLAN I. BASBAUM¶, STEVEN R. VIGNA§, AND JOHN E. MAGGIO||

*Molecular Neurobiology Laboratory (151), Veterans Administration Medical Center, Minneapolis, MN 55417; †Department of Psychiatry, University of Minnesota, Minneapolis, MN 55455; §Departments of Cell Biology, Medicine, and Surgery, Duke University Medical Center, Durham, NC 27710; ¶Departments of Anatomy and Physiology and W. N. Keck Foundation for Integrative Neuroscience, University of California, San Francisco, CA 94143; and ||Department of Biological Chemistry and Molecular Pharmacology, Harvard Medical School, Boston, MA 02115

Communicated by John R. Pappenheimer, Cambridge, MA, November 18, 1994 (received for review September 20, 1994)

ABSTRACT **Studies on cultured cells have shown that agonists induce several types of G protein-coupled receptors to undergo internalization. We have investigated this phenomenon in rat striatum, using substance P (SP)-induced internalization of the SP receptor (SPR) as our model system. Within 1 min of a unilateral striatal injection of SP in the anesthetized rat, nearly 60% of the SPR-immunoreactive neurons within the injection zone display massive internalization of the SPR—i.e., 20–200 SPR⁺ endosomes per cell body. Within the dendrites the SPR undergoes a striking translocation from the plasma membrane to endosomes, and these dendrites also undergo a morphological reorganization, changing from a structure of rather uniform diameter to one characterized by large, swollen varicosities connected by thin fibers. In both cell bodies and dendrites the number of SPR⁺ endosomes returns to baseline within 60 min of SP injection. The number of neurons displaying substantial endosomal SPR internalization is dependent on the concentration of injected SP, and the SP-induced SPR internalization is inhibited by the nonpeptide neurokinin 1 receptor antagonist RP-67,580. These data demonstrate that in the central nervous system *in vivo*, SP induces a rapid and widespread SPR internalization in the cell bodies and dendrites and a structural reorganization of the dendrites. These results suggest that many of the observations that have been made on the internalization and recycling of G protein-coupled receptors in *in vitro* transfected cell systems are applicable to similar events that occur in the mammalian central nervous system *in vivo*.**

GTP-binding regulatory protein-coupled (G protein-coupled) receptors are a large family of receptors that is widely distributed in the mammalian central nervous system (CNS). This family includes the adrenergic, dopaminergic, and all known peptidergic receptors. Although these receptors exhibit substantial diversity in the ligands with which they interact and the types of neurons and glia that express them, receptors in this family share several common structural and functional features (1, 2). All members of this family contain seven transmembrane domains and activate second-messenger systems via G proteins. Functionally, the majority of receptors in this family undergo desensitization after receptor signaling. Studies on cultured cells transfected with cDNA encoding G protein-coupled receptors indicate that after binding, several types of G protein-coupled receptors undergo phosphorylation, endosomal internalization, dissociation from the ligand in the endosome, dephosphorylation, and finally receptor recycling to the plasma membrane (3–7). Whether G protein-coupled receptors undergo a similar sequence of events *in vivo* is not known.

Substance P (SP) belongs to the tachykinin neuropeptide family which also includes neurokinin A and neurokinin B, and all tachykinins are characterized by the C-terminal sequence -Phe-Xaa-Gly-Leu-Met-NH_2 (8). In the CNS, SP is widely distributed and is present in high concentrations in the striatum, brainstem, and spinal cord. SP binds with nanomolar affinity to the SP receptor (SPR), a G protein-coupled receptor that is also known as the neurokinin 1 (NK-1) receptor (9). The SPR is also widely distributed in the brain and has been implicated in signaling nociception in the spinal cord (10) and in the modulation of cortical and striatal cell function (11).

In vivo electrophysiological studies demonstrate that neurons that express SPR undergo a rapid desensitization in response to SP (8). Radiolabeled SP is internalized in anterior pituitary cells (12) and in pancreatic acinar cells (13). In an epithelial cell line transfected with SPR cDNA, SP and the SPR are internalized into early endosomes within minutes of binding, SP is degraded in an acidified cellular compartment, and the SPR is recycled back to the cell membrane (14, 15).

Here we examine whether SP evokes internalization of SPR in the CNS *in vivo*, the time course of this internalization, the location within the neurons where this internalization occurs, the cytoplasmic localization of the internalized SPR, and whether the kinetics of the internalization are compatible with G protein-coupled receptor recycling after receptor signaling.

MATERIAL AND METHODS

Preparation of Antiserum. The antiserum was raised against a 15-aa peptide sequence at the C terminus of the rat SPR [SPR-(393–407)]. The immunogen consisted of the synthetic peptide conjugated to bovine thyroglobulin by glutaraldehyde. The antiserum recognizes a protein band of 80–90 kDa on Western blots of membranes prepared from cells transfected with the rat SPR (16). The cells were immunostained with the antiserum and the staining was blocked by preadsorbing the antiserum with SPR-(393–407).

Injections of SP, SP Antagonists, Neurokinin A, or Neurokinin B. Male Sprague–Dawley rats (240–260 g) were deeply anesthetized with sodium pentobarbital (60 mg/kg). The anesthetized rats were mounted in a small-animal stereotaxic instrument and injections were made stereotaxically into the striatum with a 28-gauge needle. The vehicle was artificial cerebrospinal fluid (128.6 mM NaCl/2.6 mM KCl/2.0 mM $MgCl_2$/1.4 mM $CaCl_2$) containing 0.1% bovine serum albumin (pH 7.4, 22°C), injected at a rate of 1 μl/min for 5 min, with

The publication costs of this article were defrayed in part by page charge payment. This article must therefore be hereby marked "*advertisement*" in accordance with 18 U.S.C. §1734 solely to indicate this fact.

Abbreviations: CNS, central nervous system; SP, substance P; SPR, SP receptor; SPR-ir, SPR immunoreactivity.
‡To whom reprint requests should be addressed.

the exception of the 1-min time point, where 5 μl of 10^{-8} M SP was injected over 30 sec. Control injections were made into the contralateral striatum. Fifteen rats received injections of 10^{-6} M SP in one striatum and either vehicle alone (5 rats), needle placement alone (5 rats), or 10^{-4} M RP-67,580 (5 rats) in the contralateral striatum. To examine whether a selective nonpeptide SPR antagonist could block SP-evoked SPR internalization, 5 rats received unilateral injection of 10^{-4} M RP-67,580 followed 10 min later by an injection of 10^{-8} M SP in the same site. To examine the time course of SP-evoked SPR internalization, 12 rats were injected with 10^{-8} M SP and allowed to survive from 30 sec to 24 hr after the injection. To examine the specificity and dose dependency of tachykinin-induced SPR internalization, 36 rats were injected unilaterally with either 10^{-10}, 10^{-8}, 10^{-6} or 10^{-4} M SP, neurokinin A, or neurokinin B (3 rats at each dose for each tachykinin) and the animals were sacrificed 5 min after injection.

Immunohistochemical Examination of the SPR. After the appropriate survival time the rats were perfused through the ascending aorta with 100 ml of 0.1 M phosphate-buffered saline (PBS; 154 mM NaCl/5.7 mM Na_2HPO_4/0.9 mM KH_2PO_4, pH 7.4, 22°C) followed by PBS/10% formaldehyde (pH 7.4, 4°C). After perfusion the brain was removed, blocked in the transverse plane, postfixed in PBS/10% formaldehyde (pH 7.4, 4°C, 6 hr), and placed in PBS/30% sucrose (pH 7.4, 4°C, 24 hr). The brains were then serially sectioned (60 μm) on a sliding microtome and collected in PBS. The sections were washed three times in PBS/1% normal goat serum/0.1% saponin (pH 7.4, 22°C) and then incubated for 12 hr in this solution containing the anti-SPR antibody (no. 11884-5) at 1:5000 (pH 7.4, 22°C). The tissue sections were then washed for 30 min at 22°C in PBS (pH 7.4) and incubated with secondary antibody solution (pH 7.4) for 2 hr at 22°C. This solution was identical to the primary antibody solution except that cyanine (Cy3)-conjugated donkey anti-rabbit IgG (no., 711-165-152; Jackson ImmunoResearch) was present (1:600) instead of anti-SPR. Finally, the tissue sections were washed for 20 min in PBS (pH 7.4, 22°C), mounted onto gelatin-coated slides, and coverslipped in PBS/90% glycerol containing 1% *p*-phenylenediamine to reduce photobleaching. For immunogold light microscopy and electron microscopy the tissue was processed as described (17, 18).

Measuring the Spread of the Injected SP. To quantify SPR internalization, we first determined the effective spread of the injected SP. This was done by performing the same stereotaxic injections as described above, except that we added 100,000 cpm of [^{125}I]Bolton–Hunter reagent-labeled SP to 5 μl of 10^{-8} M SP. This solution was injected over 5 min, the rat was sacrificed 5 min later, the brain was processed for autoradiography (9), and the slide-mounted tissue sections were placed in apposition to β-max Hyperfilm (Amersham) alongside ^{125}I-Microscales (Amersham). After 5–7 days the film was developed in Kodak D-19 developer, fixed, and washed. The autoradiograms were analyzed by quantitative densitometry with a computerized image analysis program (NIH IMAGE 1.51). We determined that a uniformly high concentration of ^{125}I-SP was present 2.0 mm on either side of the needle tract. Using this as an estimate of the effective spread of SP after injection, we sampled neurons within 1.0 mm of the needle tract.

Quantifying the Number and Extent of SPR Internalization. To examine the sites of internalization within the cell, sections were examined with an MRC-500 confocal imaging system (Bio-Rad) and an Olympus BH-2 microscope equipped for epifluorescence. Both microscopes were set up as described (18, 19).

To determine the percentage of neurons showing intense internalization, sections were examined at ×600 with a Leitz Orthoplan II microscope equipped for fluorescence. Any cell showing >20 SPR$^+$ endosomes per cell body was operationally defined as having undergone significant SPR internalization. To determine the total number of cell bodies showing SPR$^+$ internalization within 1.0 mm on either side of the injection needle tract, immunostained sections were viewed through a 1.0-cm^2 eyepiece grid, which was divided into units of 1 mm × 1 mm, and the total number of SPR$^+$ cell bodies and the number of SPR$^+$ cell bodies showing significant SPR$^+$ internalization were counted.

Statistical Analysis. Results are expressed as mean ± SEM. Differences between groups were examined by ANOVA and Student's *t* test run on STATWORKS (Computer Associates, San Jose, CA). $P < 0.05$ was considered statistically significant.

RESULTS

Cellular Distribution of SPR Immunoreactivity (SPR-ir) in Normal Striatum. In normal unstimulated rat striatum, SPR-ir is expressed in 5–10% of medium and large aspiny neurons (Figs. 1*A* and 2*A*). In the cell bodies most SPR-ir is concentrated on the neuronal membrane, effectively outlining the

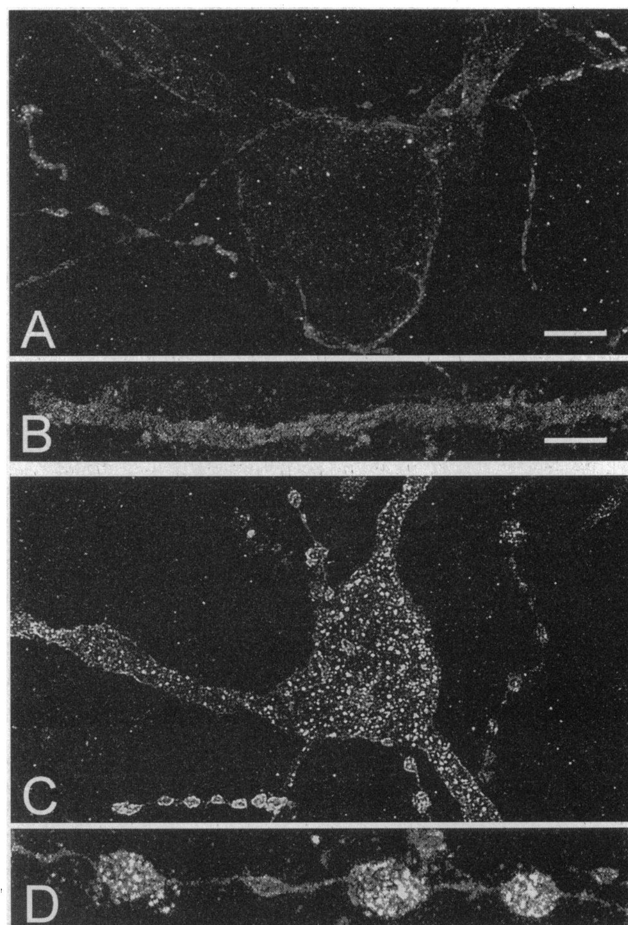

FIG. 1. SP-induced internalization of SPR-ir and morphological reorganization of dendrites in striatal neurons. Digitized confocal images show striatal neurons after injection of vehicle (*A* and *B*) and after injection of SP (*C* and *D*). The fluorescently labeled SPR-ir appears white. In an unstimulated striatal neuron (*A*) most of the SPR-ir is associated with the surface of the neuron, and few intracellular SPR$^+$ endosomes are visible. However, 5 min after injection of 5 μl of 10^{-8} M SP (*C*), a striatal neuron shows a loss of SPR-ir from the cell surface and a massive increase in intracellular SPR$^+$ endosomes (>100 endosomes per cell body). *B* and *D* show dendrites of striatal neurons after injection of vehicle (*B*) or SP (*D*). In addition to the internalization of SPR-ir within the varicosities, there is also a morphological reorganization, changing the dendrites from roughly cylindrical structures to ones characterized by large, swollen varicosities connected by thin segments. (Bar in *A* = 30 μm in *A* and *C*; bar in *B* = 10 μm in *B* and *D*).

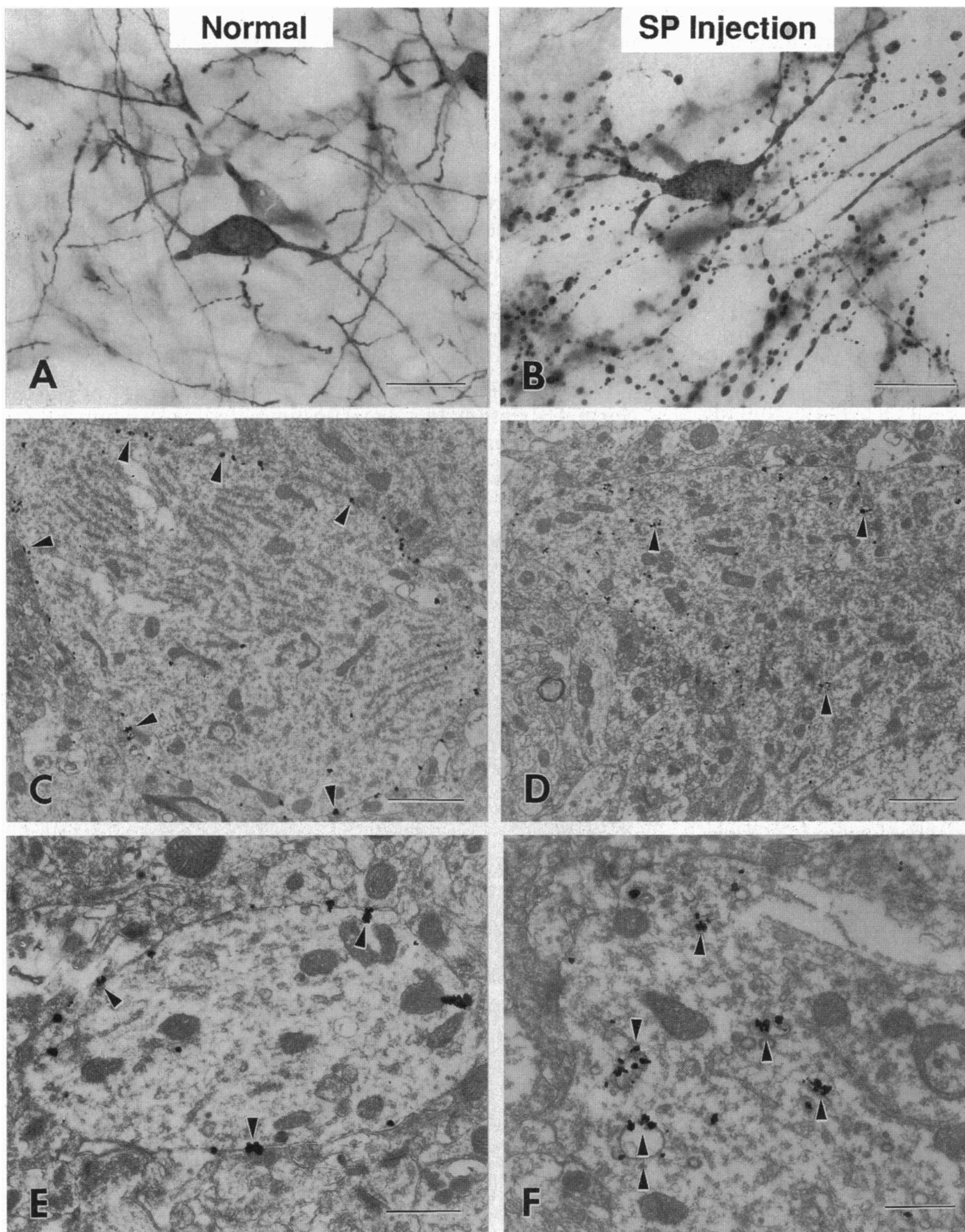

FIG. 2. Translocation of the SPR from the outer cell membrane into intracellular endosomes. Silver-enhanced immunogold bright-field micrographs (*A* and *B*) and electron micrographs (*C–F*) show the morphology of SPR$^+$ neurons and their dendrites in the unstimulated striatum (*A*, *C*, and *E*) and in the contralateral stimulated striatum (*B*, *D*, and *F*) 5 min after injection of 5 μl of 10^{-8} M SP. SPR-ir appears as dark particles. At the light microscope level, after SP injection (*B*), there is marked increase in the number and staining intensity of the SPR$^+$ dendritic varicosities compared with the unstimulated striatum (*A*). The electron micrographs (*C–F*) show SPRs, identified by dark, electron-dense colloidal gold particles (arrowheads), undergoing translocation from the plasma membrane into the cytoplasm in the cell body (*C* and *D*) and dendrites (*E* and *F*). [Bars = 100 μm (*A* and *B*), 1 μm (*C* and *D*), or 0.5 μm (*E* and *F*).]

labeled neurons (Figs. 1*A* and 2 *A*, *C*, and *E*). In addition, a relatively small amount of SPR-ir is present intracellularly in endosomes (0.1–0.7 μm in diameter), with most SPR$^+$ striatal neurons having <5 SPR$^+$ endosomes per cell body and none having >20 endosomes per cell body (Figs. 1*A* and 3*A*). At the light microscopic level, we defined an endosome as any intracellular organelle 0.1–0.7 μm in diameter that showed intense SPR-ir.

In the dendrites of SPR$^+$ neurons, SPR-ir is rather homogeneously associated with the neuronal plasma membrane (Fig. 1*B*). However, in ≈5% of the SPR$^+$ distal dendrites, intense SPR-ir is also associated with varicosities. Within these SPR-immunoreactive varicosities, clustering of SPR-immunoreactive endosomes can be seen (Fig. 1*D*). Although SPR$^+$ endosomes are also occasionally observed in the non-varicose dendrites, the concentration of SPR$^+$ endosomes within the nonvaricose segments is much lower than that observed in the varicosities.

Internalization of SPR in Cell Bodies After SP Injection. The distribution of SPR-ir in the striatum is markedly altered after injection of 10^{-8} M SP (Figs. 1*C*, 2*B*, and 3*B*). One minute after SP injection nearly 60% of the SPR$^+$ neurons within the injection zone (<1.0 mm from the needle tract) exhibit internalization of SPR (>20 SPR$^+$ endosomes per cell body; Fig. 4). These SPR$^+$ endosomes are 0.1–0.7 μm in diameter and the increase in the number of SPR$^+$ endosomes per cell body is accompanied by a substantial *decrease* in the SPR-ir associated with the plasma membrane of the same neuron as seen by electron microscopy (Fig. 2*C* vs. 2*D* and Fig. 2*E* vs. 2*F*). Not all SPR$^+$ cells within the 1.0-mm injection zone exhibit a substantial increase in SPR$^+$ endosomal internalization. Neurons that demonstrate an increase in endosomal SPR-ir within their cell bodies can be found adjacent to neurons that have surface SPR-ir, with no increase in SPR$^+$ endosomes.

Control experiments included placing the injection needle into the striatum for 5 min without any injection, injection of vehicle alone, and injection of 5 μl of 10^{-8} or 10^{-4} M RP-67,580 alone. None of these injections significantly altered the distribution of SPR-ir in SPR$^+$ neurons, either inside or outside the zone of injection. We also injected 10^{-4} M RP-67,580 followed 10 min later by an injection of 10^{-8} M SP. Prior injection of the nonpeptide SPR antagonist produced a >80% reduction in the number of striatal neurons showing significant SPR internalization.

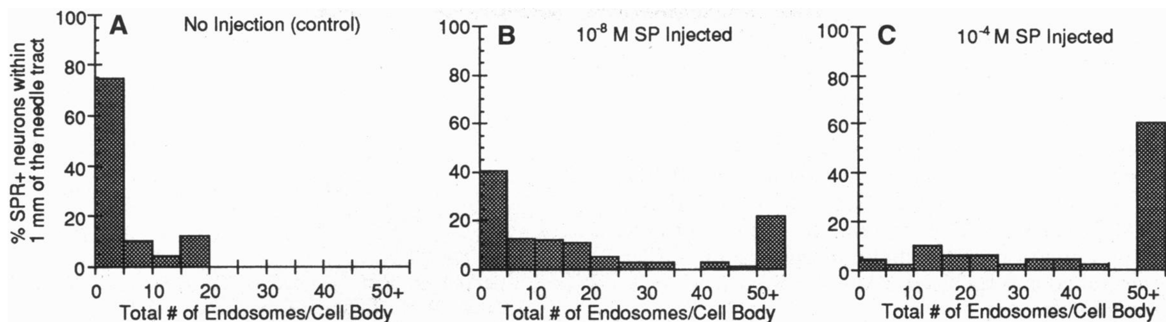

FIG. 3. Number of SPR$^+$ endosomes per cell body in neurons in the normal striatum (*A*) and in the striatum 5 min after 10^{-8} M (*B*) or 10^{-4} M (*C*) SP injection. By confocal optic sectioning, counts were made of the total number of SPR$^+$ endosomes per cell body in neurons within 1 mm of the injection zone, which was determined by examining the spread of ^{125}I-SP.

Internalization of SPR in Dendrites after SP Injection. The most striking SP-induced change in SPR$^+$ striatal neurons occurs in the distal dendrites (Figs. 1*D* and 2*B*). Injection of SP induces SPR internalization as well as a structural reorganization of the dendrites. Normal SPR$^+$ distal dendrites have a rather uniform diameter, with SPR-ir essentially outlining the outer cell membrane (Figs. 1*B* and 2*A*). One minute after injection of 10^{-8} M SP, the majority of SPR$^+$ dendrites appear as large, swollen varicosities connected by thin fibers which are <20% the diameter of the swollen varicosities (Figs. 1*D* and 2*B*). Thus, at low power each dendrite now appears as a chain of intense SPR-immunoreactive varicosities, without an obvious intervening connecting fiber (Fig. 2*B*). At high magnification it is evident that the swollen, intensely SPR-immunoreactive varicosities are packed with SPR$^+$ endosomes, whereas the thin fibers that connect these varicosities are devoid of endosomes (Fig. 1*D*).

Time Course of SPR Internalization After SP Injection. The initial increase and subsequent decrease in SP-induced SPR$^+$ endosomes are very rapid. One minute after injection of 10^{-8} M SP nearly 60% of the labeled neurons within the injection zone exhibit SPR internalization (Fig. 4). Equally dramatic is how quickly the number of SPR$^+$ endosomes per cell body decreases. Thirty minutes after SP injection, <10% of SPR$^+$ neuronal cell bodies show significant SPR$^+$ internalization. In parallel with this increase and subsequent decrease in endosomal SPR-ir are a decrease and increase, respectively, in the SPR-ir associated with the plasma membrane. Thus, as the concentration of intracellular endosomal SPR-ir increases, there is a concomitant decrease in SPR-ir associated with the outer cell membrane.

SP-Evoked Internalization of SPR in Both Neurons and Dendrites Is Dose-Dependent and SP-Specific and Is Blocked by the Nonpeptide SPR Antagonist RP-67,580. Control experiments show that the SP-induced internalization of the SPR is dose-dependent, with an EC_{50} of 0.93 nM. The EC_{50} is 21 nM for neurokinin A and >1.0 μM for neurokinin B. These EC_{50} values correspond closely to the affinities of these peptides at the rat SPR (9). SPR internalization appears to be due to receptor activation rather than simple ligand binding, since injection of 5 μl of 10^{-4} M RP-67,580, which also binds the SPR, but at a different site than SP (20), produces no significant internalization of the SPR.

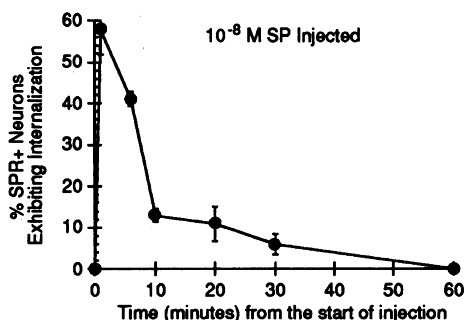

FIG. 4. Time course of SPR$^+$ internalization after injection of 10^{-8} M SP into the striatum. Neuronal cell bodies that contained >20 endosomes per cell body are considered to have internalized the SPR. Maximal internalization is observed 1 min after injection, the earliest time point examined.

DISCUSSION

This report demonstrates that in the rat CNS *in vivo*, a prototypical G protein-coupled receptor, the SPR (NK-1 receptor) undergoes rapid internalization in response to binding to its native agonist. The SP-evoked internalization occurs in both the cell body and the dendrites. Since the increase in endosomal SPR is paralleled by a loss of SPR-ir in the plasma membrane of both the cell body and dendrites, it is likely that the majority of the internalized SPR arises from the SPR that is present in the neuronal plasma membrane. Our data also suggest that the SPRs, which are present at both synaptic specializations and "nonsynaptic" sites (18), are functional, since SPRs at both sites undergo rapid internalization after agonist binding.

Our results provide insight not only into the mechanisms of SP-induced SPR internalization but also into those of several other G protein-coupled receptors. From data generated largely in studies on cultured cells transfected with cDNA encoding a G protein-coupled receptor and thus expressing high concentrations of the receptor, the following features of G protein-coupled receptors that undergo internalization have begun to emerge (4–7). After the initial agonist–receptor interaction, which induces signal transduction, G protein-coupled receptors undergo phosphorylation, endosomal internalization, dissociation from the ligand in the endosome, dephosphorylation, and finally receptor recycling back to the plasma membrane. After agonist exposure there is frequently a relatively long period (2–60 min) of tachyphylaxis—i.e., further application of the agonist does not evoke receptor signaling. This is followed by gradual receptor resensitization.

The phosphorylation of several G protein-coupled receptors, including the SPR and the β_1-, and β_2-adrenergic receptors, is mediated by a β-adrenergic receptor kinase (21, 22). Receptor phosphorylation, at least for the β_2 receptor, appears to be responsible for initial acute homologous desensitization. After signal transduction, this entire phosphorylated ligand–receptor complex is internalized into acidic endosomes, which is thought to facilitate dissociation of the ligand–receptor complex and dephosphorylation of the receptor, which is required for reactivation (5, 23). The rapid and massive internalization of the SPR may also contribute to the desensitization of the receptor; sequestering the receptor makes it physically inaccessible to extracellular hydrophilic agonists.

Our results show that the rapid internalization of the SPR is paralleled by a loss of SPR-ir from the cell surface and that within 30 min after agonist challenge, the majority of the SPR-ir has reappeared at the cell surface. Given the time required for new protein synthesis, the massive translocation of the receptor that occurs after occupancy by SP, and the previous demonstration of receptor recycling in an epithelial cell system (14), our results strongly suggest that the majority of the internalized SPRs *in vivo* are ultimately recycled to the plasma membrane after endosomal internalization, rather than being degraded and replaced in the membrane by newly synthesized receptors.

A previous study provided light microscopic and ultrastructural evidence that SPR-ir is present along the majority of the neuronal outer cell membrane, in both the cell body and the dendrites (18). This relatively uniform distribution of SPRs along the plasma membrane is in sharp contrast to the rather strict synaptic localization observed for some glutamate (24, 25) or glycine (26, 27) receptors which are members of the ligand-gated ion-channel receptor family. In response to receptor binding, several members of the ligand-gated ion-channel family undergo receptor clustering at specific sites in the outer cell membrane rather than internalization (28). This is in sharp contrast to the present results, which show that in the case of the G protein-coupled SPR, *in vivo* endosomal internalization occurs in all parts of the cell where the SPR is normally present, including every dendrite that the agonist appears to have reached.

The concept that activation of a G protein-coupled receptor can produce a structural reorganization of the dendrite within minutes of ligand–receptor interaction is concordant with observations suggesting that neurons display substantial synaptic plasticity following stimulation (29, 30). Our data also suggest that the internalization and structural reorganization that occurs in response to an agonist should alter the electrophysiological properties of the stimulated dendrite. Aside from the inaccessibility of the internalized receptor to hydrophilic extracellular agonists, the striking changes in the morphology of the dendrites should alter the passive electrical properties of the dendrite (31). Our results may be important in linking neurochemical events to long-term changes in cell morphology, since repeated receptor activation has been reported to produce long-term cytoskeletal changes (32). Just what is unique about the dendritic sites at which varicosities occur is unclear, but our results imply that there must be a cytoskeletal framework to guide the receptor to the varicosity and then back again to the outer cell membrane.

In summary, our results suggest that rapid receptor internalization of G protein-coupled receptors occurs in the CNS *in vivo* in response to agonist binding. Particularly striking is the rapid time course of both the initial appearance and subsequent disappearance of the internalized SPR. This massive internalization is accompanied by a structural reorganization of the distal dendrites. Given the extent and speed of the translocation of these receptors, we suggest that the ultimate fate of the majority of the internalized receptors is recycling rather than degradation. We hypothesize that the present results are applicable to several other G protein-coupled receptors and that many of the findings concerning G protein-coupled receptor internalization and recycling that have been made in *in vitro* systems are directly applicable to the CNS *in vivo*.

We thank C. Garret (Rhone-Poulenc-Rorer) for a gift of RP-67580. This work was supported by National Institutes of Health Grants NS23970, AG11852, NS21445, NS14627, GM15904, and DA08973 and a Veterans Administration Merit Review.

1. Lefkowitz, R. J. & Caron, M. G. (1990) *Adv. Second Messenger Phosphoprotein Res.* **24**, 1–8.
2. Collins, S., Caron, M. G. & Lefkowitz, R. J. (1992) *Trends Biochem. Sci.* **17**, 37–39.
3. Senogles, S. E., Spiegel, A. M., Padrell, E., Iyengar, R. & Caron, M. G. (1990) *J. Biol. Chem.* **265**, 4507–4514.
4. Caron, M. G. & Lefkowitz, R. J. (1993) *Recent Prog. Horm. Res.* **48**, 277–290.
5. Lefkowitz, R. J., Cotecchia, S., Kjelsberg, M. A., Pitcher, J., Koch, W. J., Inglese, J. & Caron, M. G. (1993) *Adv. Second Messenger Phosphoprotein Res.* **28**, 1–9.
6. Kobilka, B. (1992) *Annu. Rev. Neurosci.* **15**, 87–114.
7. Von Zastrow, M., Link, R., Daunt, D., Barsh, G. & Kobilka, B. (1993) *J. Biol. Chem.* **268**, 763–766.
8. Maggio, J. E. (1988) *Annu. Rev. Neurosci.* **11**, 13–28.
9. Mantyh, P. W., Gates, T., Mantyh, C. R. & Maggio, J. E. (1989) *J. Neurosci.* **9**, 258–279.
10. De Koninck, Y. & Henry, J. L. (1991) *Proc. Natl. Acad. Sci. USA* **88**, 11344–11348.
11. Mantyh, P. W., Pinnock, R. D., Downes, C. P., Goedert, M. & Hunt, S. P. (1984) *Nature (London)* **309**, 795–797.
12. Reubi, J. C., Kvols, L., Krenning, E. & Lamberts, S. W. J. (1990) *Metabolism* **39** (Suppl. 2), 78–81.
13. Sjodin, L., Brodin, E., Nilsson, G. & Conlon, T. P. (1980) *Acta Physiol. Scand.* **109**, 97–105.
14. Garland, A. M., Grady, E. F., Payan, D. G., Vigna, S. R. & Bunnett, N. W. (1994) *Biochem. J.* **303**, 177–186.
15. Bowden, J. J., Garland, A. M., Baluk, P., Lefevre, P., Grady, E. F., Vigna, S. R., Bunnett, N. W. & McDonald, D. M. (1994) *Proc. Natl. Acad. Sci. USA* **91**, 8964–8968.
16. Vigna, S. R., Bowden, J. J., McDonald, D. M., Fisher, J., Okamoto, A., McVey, D. C., Payan, D. G. & Bunnett, N. W. (1994) *J. Neurosci.* **14**, 834–845.
17. Sasek, S. R., Aoki, C. & Pickel, V. M. (1994) *J. Neurosci.* **14**, 88–106.
18. Liu, H., Brown, J. L., Jasmin, L., Maggio, J. E., Vigna, S. R., Mantyh, P. W. & Basbaum, A. I. (1994) *Proc. Natl. Acad. Sci. USA* **91**, 1009–1013.
19. Mantyh, P. W., Rogers, S. D., Allen, C. J., Catton, M. D., Ghilardi, J. R., Levin, L. A., Maggio, J. E. & Vigna, S. R. (1995) *J. Neurosci.* **15**, 152–164.
20. Moussaoui, S. M., Montier, F., Carruette, A., Blanchard, J. C., Laduron, P. M. & Garret, C. (1993) *Br. J. Pharmacol.* **109**, 259–264.
21. Kwatra, M. M., Schwinn, D. A., Schreurs, J., Blank, J. L., Kim, C. M., Benovic, J. L., Krause, J. E., Caron, M. G. & Lefkowitz, R. J. (1993) *J. Biol. Chem.* **268**, 9161–9164.
22. Inglese, J., Luttrell, L. M., Iñiguez-Lluhi, J. A., Touhara, K., Koch, W. J. & Lefkowitz, R. J. (1994) *Proc. Natl. Acad. Sci. USA* **91**, 3637–3641.
23. Yu, S. S., Lefkowitz, R. J. & Hausdorff, W. P. (1993) *J. Biol. Chem.* **268**, 337–341.
24. Petralia, R. S., Yokotani, N. & Wenthold, R. J. (1994) *J. Neurosci.* **14**, 667–696.
25. Petralia, R. S. & Wenthold, R. J. (1992) *J. Comp. Neurol.* **318**, 329–354.
26. Naas, E., Zilles, K., Gnahn, H., Betz, H., Becker, C. M. & Schroder, H. (1991) *Brain Res.* **561**, 139–146.
27. Betz, H. (1991) *Trends Neurosci.* **14**, 458–461.
28. Kirsch, J., Wolters, I., Triller, A. & Betz, H. (1993) *Nature (London)* **366**, 745–748.
29. Woolf, C. J. (1983) *Nature (London)* **306**, 686–688.
30. Dubner, R. (1991) in *Proceedings of VI World Congress on Pain: Pain Research and Clinical Management*, eds. Bond, M., Charlton, E. & Woolf, C. J. (Elsevier, Amsterdam), Vol. 5, pp. 263–276.
31. Jack, J. (1979) in *The Neurosciences: Fourth Study Program*, eds. Schmitt, F. O. & Worden, F. G. (MIT Press, Cambridge, MA), pp. 423–437.
32. Mitchison, T. & Kirschner, M. (1988) *Neuron* **1**, 761–772.